Direct verification of mixing rules in the hot and dense regime

F. Lambert, J. Clérouin, J.-F. Danel, L. Kazandjian,* and G. Zérah
Commissariat à l'Energie Atomique, Centre DAM Ile-de-France, Bruyères-le-Châtel, 91297 Arpajon Cedex, France
(Received 13 November 2007; published 4 February 2008)

We perform orbital-free molecular dynamics simulations in the hot and dense regime for two mixtures: equimolar helium-iron and asymmetric deuterium-copper plasmas. For thermodynamic properties, we test two isobaric-isothermal mixing rules whose definitions involve either the equality of total pressures or the equality of the so-defined excess pressures of the components; the pressure and internal energy obtained by direct simulations are in very good agreement with those given by the mixing rule involving the equality of excess pressures. The viscosity of the deuterium-copper mixture is also extracted from a direct simulation and compared to the result given by a mixing rule applied to the viscosities of the pure elements. Finally, for structural properties, the effective charges given by the isobaric-isothermal mixing rule for the average atom model, used in the binary ionic mixture model, yield partial pair distribution functions in good agreement with those obtained by a direct simulation.

DOI: 10.1103/PhysRevE.77.026402 PACS number(s): 52.65.−y, 52.25.Kn, 52.25.Fi

I. INTRODUCTION

Mixtures are often encountered in both astrophysical plasmas and inertial confinement fusion (ICF) plasmas. Their properties are of prime importance for "scientific" as well as "technological" issues. For example, the equation of state (EOS) gives an insight into the possibility of phase separation which remains an open question for hydrogen and helium inside giant planets [1–3]. The transport coefficients of mixtures are also particularly relevant for hydrodynamic simulations in ICF; for example, viscosity governs the growth of hydrodynamic instabilities [4]. This quantity has been recently studied for an asymmetric mixture of deuterium and gold in the framework of the binary ionic mixture (BIM) [5] where ions interact by a pure Coulombic potential. Unfortunately, this model relies on knowledge of the effective charges of the components of the mixture, quantities that have to be determined by an *ad hoc* prescription.

Contrary to this parametrized model, first-principles simulations, like quantum molecular dynamics, allow one to directly deal with mixtures without any *ad hoc* prescription. Such simulations turned out to account for experimental EOS and optical properties of diluted aluminum and gold plasmas [6]. Yet the quantum description of electrons becomes numerically intractable as temperature or density increases. Indeed, as temperature grows, the number of electronic quantum states to be taken into account is colossal due to the Fermi-Dirac distribution of electrons. In order to address the high-temperature regime, we proposed an alternative scheme in which electrons were no longer described by orbitals, as in quantum molecular dynamics, but by a free-energy functional depending only on the local electronic density. This approach, orbital-free molecular dynamics (OFMD), has been found valid at high density for boron [7] and can be used to deal with hot and dense plasmas of high-atomic-number elements [8–10]. For hydrodynamics, it is of practical interest to find mixing rules allowing one to predict the properties of a mixture from the properties of its pure components. Mixing rules for the equation of state have been studied in the framework of specific models like the BIM and its extension to Yukawa-type plasmas [11–14]. In the present paper, we test the mixing rules in the hot and dense regime thanks to direct simulations of the mixture by OFMD; we consider the equation of state as well as the viscosity and the partial pair distribution functions.

The paper is organized as follows. Theoretical and numerical aspects of OFMD are explained in Sec. II. The isobaric-isothermal mixing rules are defined in Sec. III. They are tested for the calculation of pressure and internal energy, in Sec. IV, on an equimolar helium-iron mixture and, in Sec. V, on an asymmetric deuterium-copper mixture. In the latter case, the isobaric-isothermal mixing rules are used to calculate viscosity. Furthermore, the isobaric-isothermal mixing rule for the average atom model [15], used with the BIM model, gives good partial pair distribution functions. The OFMD simulations are performed with the electronic structure package ABINIT [16]. Atomic units are used throughout the paper if not indicated otherwise.

II. ORBITAL-FREE MOLECULAR DYNAMICS

Most *ab initio* techniques are based on coupling finite-temperature density-functional theory (DFT) [17,18] for the electrons and molecular dynamics for the nuclei by using the Born-Oppenheimer approximation. In these methods, the dynamics of the N nuclei located at $\boldsymbol{R}_i$, of mass M_i and atomic number Z_i, is driven by both electronic and nuclear Coulomb interactions and is represented by the following Lagrangian:

$$L[n(\boldsymbol{r}),\{\boldsymbol{R}_i\},\{\dot{\boldsymbol{R}}_i\}] = \frac{1}{2}\sum_{i=1}^{N} M_i \dot{\boldsymbol{R}}_i^2 - \frac{1}{2}\sum_{\substack{i,j=1 \\ i\neq j}}^{N} \frac{Z_i Z_j}{|\boldsymbol{R}_i - \boldsymbol{R}_j|} - F^e[n(\boldsymbol{r}),\{\boldsymbol{R}_i\}], \quad (1)$$

where $F^e[n(\boldsymbol{r}),\{\boldsymbol{R}_i\}]$ stands for the electronic free energy that depends only on the local electronic density $n(\boldsymbol{r})$ in the DFT formalism.

*Corresponding author: luc.kazandjian@cea.fr

In quantum molecular dynamics, the electrons are described, in the framework of DFT, by an independent-particle model which leads to the well-known Kohn-Sham equations [19]. In contrast to the Kohn-Sham method, the orbital-free approach used here directly deals with the free energy as a functional of the electronic density without introducing the one-electron Kohn-Sham orbitals. The orbital-free free energy [20] is then

$$F^e[n] = \frac{1}{\beta}\int d\boldsymbol{r}\left(n(\boldsymbol{r})\Phi[n(\boldsymbol{r})] - \frac{2\sqrt{2}}{3\pi^2\beta^{3/2}}I_{3/2}\{\Phi[n(\boldsymbol{r})]\}\right) + \int d\boldsymbol{r}\, V(\boldsymbol{r})n(\boldsymbol{r}) + \frac{1}{2}\int\int d\boldsymbol{r}\, d\boldsymbol{r}'\frac{n(\boldsymbol{r})n(\boldsymbol{r}')}{|\boldsymbol{r}-\boldsymbol{r}'|} + F^{xc}[n], \tag{2}$$

where β is the inverse of the temperature, I_α is the Fermi function of order α, $V(\boldsymbol{r})$ is the external potential—i.e., the ionic Coulombic potential or a regularized potential—and $F^{xc}[n]$ is the exchange-correlation term chosen to be the local-density approximation of Perdew and Zunger [21]. The screened potential $\Phi[n(\boldsymbol{r})]$ is related to the electronic density $n(\boldsymbol{r})$ through

$$n(\boldsymbol{r}) = \frac{\sqrt{2}}{\pi^2\beta^{3/2}}I_{1/2}\{\Phi[n(\boldsymbol{r})]\}. \tag{3}$$

If exchange-correlation is neglected, $F^e[n]$ in Eq. (2) is nothing but the Thomas-Fermi functional at finite temperature. We emphasize again that the nuclei are characterized only by their atomic number Z_i and their mass M_i so that pure elements and mixtures are treated on an equal footing.

At each time step, for given $\boldsymbol{R}_i$'s, the free energy is minimized with respect to the local electronic density under the constraint of charge neutrality of the mixture. The forces acting on the nuclei are then computed from the electronic density and the nuclei are moved in the isokinetic ensemble [22,23] (other statistical ensembles, like the microcanonical one, could be used, but the isokinetic ensemble allows one to regard temperature as exactly known). In practice, the nucleus-electron interactions are regularized potentials instead of the bare Coulombic potential [8]; they are no longer Coulombic below a given cutoff radius (one for each type of nucleus). Convergence studies must ensure that the resulting quantities do not depend, within about one standard deviation, on the regularization. The choice of the cutoff radii and of the other simulation parameters is explained in Appendix A.

III. ISOBARIC-ISOTHERMAL MIXING RULES

A mixing rule for an equation of state allows one to calculate the equation of state of a mixture from the equation of state of its components (and the mole fractions). An isobaric-isothermal mixing rule has been defined in the framework of the average atom model [15], but has not been verified so far. We define similar mixing rules, designated by MR1 and MR2, to calculate the excess pressure P_{ex} and the excess internal energy per atom, E_{ex}, of a mixture at density ρ and temperature T. These quantities are defined as follows:

$$P_{ex} = P - n_I kT, \tag{4}$$

$$E_{ex} = E - \frac{3}{2}kT, \tag{5}$$

where P and E are the total pressure and the internal energy per atom, k is the Boltzmann constant, and n_I is the number of nuclei per unit volume.

In our definition of MR1, the partial densities ρ_ℓ related to component ℓ are determined by the following two equations: (i) equality of the excess pressures of the pure components ℓ at their respective partial densities and at temperature T,

$$P_{ex,\ell}(\rho_\ell, T) = P_{ex,m}(\rho_m, T), \quad \forall \quad \ell, m, \tag{6}$$

and (ii) additivity of partial volumes,

$$\frac{1}{\rho}\sum_\ell x_\ell A_\ell = \sum_\ell x_\ell \frac{A_\ell}{\rho_\ell}, \tag{7}$$

where A_ℓ and x_ℓ are the atomic mass and the mole fraction of component ℓ.

It is implicitly supposed that there is a one-to-one relationship between density and pressure in Eq. (6) so that Eqs. (6) and (7) have a unique solution. Once the ρ_ℓ's are known, the excess pressure is taken equal to the $P_{ex,\ell}$'s of Eq. (6) and the excess internal energy per atom is taken equal to

$$E_{ex}(\rho, T, \{x_\ell\}) = \sum_\ell x_\ell E_{ex,\ell}(\rho_\ell, T), \tag{8}$$

where $E_{ex,\ell}(\rho_\ell, T)$ is the excess internal energy per atom of the pure component ℓ at density ρ_ℓ and temperature T.

We define another mixing rule, designated by MR2, by Eqs. (7) and (8) and by Eq. (9) which expresses the equality of the total pressures of the pure components ℓ at their respective partial densities ρ_ℓ and at temperature T:

$$P_\ell(\rho_\ell, T) = P_m(\rho_m, T), \quad \forall \quad \ell, m. \tag{9}$$

Once the ρ_ℓ's are determined by Eqs. (7) and (9), the total pressure of the mixture is taken equal to the P_ℓ's of Eq. (9) and the excess internal energy is calculated with Eq. (8). Choosing either excess or total pressures to define the isobaric-isothermal mixing rule relies on two different qualitative interpretations:

(i) On the one hand, one can consider a complete mixing of the two elements. In that case, each element "exchanges" electrons with the other one, a kind of chemical reaction, and the thermodynamic potential that is equalized between the two species is the chemical potential [24]. Since in the average atom framework the chemical potential determines the pressure, equality of the chemical potential leads to equality of the "electronic pressure" which is *chosen* to be the excess pressure in OFMD.

(ii) On the other hand, one can consider droplets of each species interacting with each other by "exchanging" volumes so that the thermodynamic potential equalized is the total pressure [25].

It can be shown that, given the additivity of partial volumes and the equality of either excess or total pressures, the values of the pressure and internal energy of the mixture

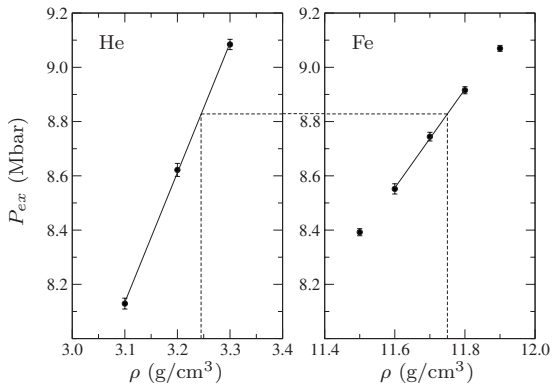

FIG. 1. Isobaric-isothermal mixing rule MR1 applied to an equimolar mixture of ^{4}He and ^{56}Fe at 10 g cm^{-3} and 5 eV. Dots represent OFMD simulations for each pure element, and solid lines are linear fits. Partial densities, given by the dashed lines, result from Eqs. (6) and (7). The position of the horizontal dashed line is determined by the rule of additivity of partial volumes. Vertical bars represent standard deviations.

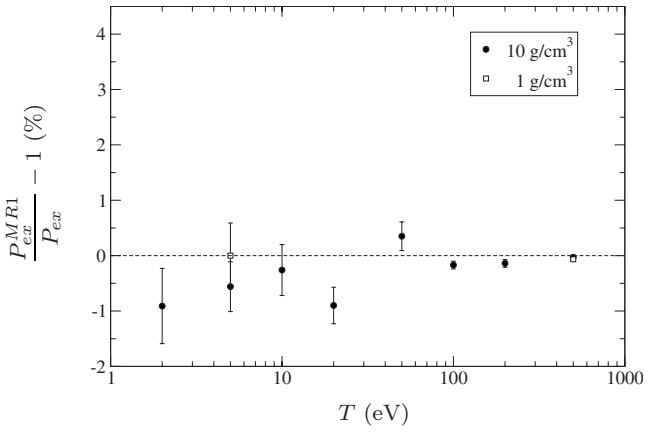

FIG. 2. Equimolar He-Fe mixture. Comparison of the excess pressures given by direct simulations (P_{ex}) and by the mixing rule MR1 (P_{ex}^{MR1}). Vertical bars represent relative standard deviations.

can be obtained by expressing either the excess or total free energy as a weighted sum; this point is discussed in Appendix B.

IV. APPLICATION TO AN EQUIMOLAR MIXTURE OF HELIUM AND IRON

We now use OFMD, either alone or in association with MR1 or MR2, to compute the pressure and internal energy of an equimolar mixture of ^{4}He (atomic mass $A=4.0026$ g mol^{-1}) and ^{56}Fe ($A=55.935$ g mol^{-1}). In Fig. 1, we have plotted a graphical scheme that illustrates the algorithm of Eqs. (6) and (7), for instance. In each direct simulation of the mixture, 30 particles (15 of each component) are propagated during 2000 time steps; for pure He or pure Fe involved in applying MR1 or MR2, 32 particles are propagated during 2000 time steps. The other numerical parameters are chosen as indicated in Appendix A. The variation of excess pressure with temperature at 1 g cm^{-3} and 10 g cm^{-3}, obtained with direct simulation or MR1 or MR2, is shown in Table I and in Figs. 2 and 3. In the thermodynamic domain covered, the electrons go from degenerate to classical. The pressures given by MR1 are in excellent agreement with those given by a direct simulation, the maximum relative error being less than 1% and less than twice the relative standard deviation. With MR2, the agreement is generally less good and all the less so as the kinetic pressure due to nuclei is a large part of the total pressure (15% at 5 eV and 10 g cm^{-3}, 1% at 500 eV and 10 g cm^{-3}, 46% at 5 eV and 1 g cm^{-3}, 8% at 500 eV and 1 g cm^{-3}).

As in the case of pure elements, because of the regularization of the nucleus-electron interaction necessary for OFMD, the internal energy is not properly computed and must be corrected with the help of the average atom model [10]. We propose to calculate the exact excess internal energy per atom, $E_{ex}(\rho,T,\{x_\ell\})$, obtained with a Coulombic nucleus-electron interaction, through

TABLE I. Excess pressure for an equimolar mixture of ^{4}He and ^{56}Fe. P_{ex}^s designates the results given by direct simulations; P_{ex}^{MR1} and P_{ex}^{MR2} designate the results given by the mixing rules MR1 and MR2 used with OFMD. The numbers in parentheses are standard deviations.

ρ (g cm^{-3})	T (eV)	P_{ex}^s	P_{ex}^{MR1} (Mbar)	P_{ex}^{MR2}
1	5	0.1854 (6×10^{-4})	0.1854 (5×10^{-4})	0.1918 (6×10^{-4})
1	500	183.97 (2×10^{-2})	183.85 (2×10^{-2})	182.58 (2×10^{-2})
10	2	6.88 (2×10^{-2})	6.82 (2×10^{-2})	6.88 (1×10^{-2})
10	5	8.88 (2×10^{-2})	8.83 (2×10^{-2})	8.95 (2×10^{-2})
10	10	13.11 (3×10^{-2})	13.07 (3×10^{-2})	13.27 (2×10^{-2})
10	20	24.21 (4×10^{-2})	24.00 (4×10^{-2})	24.40 (3×10^{-2})
10	50	70.48 (9×10^{-2})	70.73 (6×10^{-2})	71.10 (4×10^{-2})
10	100	178.51 (6×10^{-2})	178.21 (8×10^{-2})	178.60 (6×10^{-2})
10	200	466.56 (9×10^{-2})	465.93 (2×10^{-1})	465.35 (2×10^{-1})
10	500	1611.60 (3×10^{-1})	1611.10 (5×10^{-1})	1607.48 (3×10^{-1})

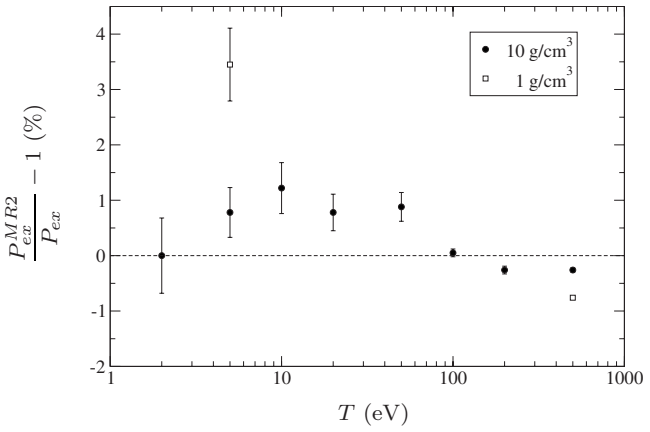

FIG. 3. Equimolar He-Fe mixture. Comparison of the excess pressures given by direct simulations (P_{ex}) and by the mixing rule MR2 (P_{ex}^{MR2}). Vertical bars represent relative standard deviations.

$$E_{ex}(\rho,T,\{x_\ell\}) = E_{ex}^{ps}(\rho,T,\{x_\ell\}) + [E_{AA}(\rho,T,\{x_\ell\}) - E_{AA}^{ps}(\rho,T,\{x_\ell\})], \tag{10}$$

where $E_{ex}^{ps}(\rho,T,\{x_\ell\})$ is the excess internal energy per atom given by the OFMD simulation for the regularized interactions considered (*ps* stands for pseudopotential) and $E_{AA}(\rho,T,\{x_\ell\})$ and $E_{AA}^{ps}(\rho,T,\{x_\ell\})$ are the internal energies per atom computed, with the average atom model and the isobaric-isothermal mixing rule [15], for the Coulombic interaction and for the regularized interactions considered.

We have observed that, as the cutoff radii are lowered, the right-hand side of Eq. (10) eventually becomes constant within one standard deviation. We conjecture that this property extends up to very small values of the cutoff radii for which the right-hand side of Eq. (10) tends to the excess internal energy sought. We therefore use Eq. (10), implemented with sufficiently small cutoff radii, to compute the excess internal energy per atom with OFMD. The results are shown in Table II where the excess internal energies given by MR1 and MR2 are compared to those given by direct simulations. Agreement between direct simulations and MR1 is very good. With MR2, the agreement is generally less good; MR2 gives results which become more different from the exact ones as temperature gets higher. This difference in the internal energies given by MR1 and MR2 stems from the difference in the partial densities obtained with each method. At low temperature, MR1 and MR2 give close results because the internal energy varies little with density; it is no longer the case at high temperature. It can be noted that, at high temperature, direct simulations give excess internal energies close to those of the average atom model; this fact confirms the interest of MR1 and of the mixing rule for the average atom model [15].

V. APPLICATION TO AN ASYMMETRIC MIXTURE: DEUTERIUM AND COPPER IN ICF CONDITIONS

In the previous section, OFMD has been applied to the computation of pressure and internal energy. These quantities are rather "easy" to calculate since their convergence with respect to the number of particles and to the number of time steps is fast. In this section, besides pressure and internal energy, we also calculate structural properties and viscosity. We consider a mixture of deuterium ($A=2.0140$ g mol^{-1}) and copper (^{63}Cu, $A=62.930$ g mol^{-1}), with respective molar fractions $x_D=0.9$ and $x_{Cu}=0.1$, at 50 g cm^{-3} and 100 eV. This mixture is inspired by the "double-shell" design of the target in ICF [26] in which, during the compression phase, the mixing of light and heavy elements can occur because of Rayleigh-Taylor instabilities [26].

In order to get a good statistics on our results, especially pair distribution functions and viscosity, we perform a simulation of the aforementioned mixture with 500 particles, 450 atoms of deuterium and 50 atoms of copper, propagated during 47 000 time steps (or 0.5 ps). This large number of time

TABLE II. Excess internal energies per atom for an equimolar mixture of ^{4}He and ^{56}Fe. E_{ex}^s designates the results given by direct simulations; E_{ex}^{MR1} and E_{ex}^{MR2} designate the results given by the mixing rules MR1 and MR2 used with OFMD. All excess internal energies are corrected with Eq. (10). The numbers in parentheses are standard deviations.

ρ (g cm^{-3})	T (eV)	E_{ex}^s	E_{ex}^{MR1} (keV/atom)	E_{ex}^{MR2}
1	5	−21.406 (1×10^{-5})	−21.406 (1×10^{-5})	−21.405 (1×10^{-5})
1	500	−6.586 (1×10^{-3})	−6.590 (1×10^{-3})	−6.639 (8×10^{-4})
10	2	−21.409 (4×10^{-5})	−21.409 (4×10^{-5})	−21.410 (2×10^{-5})
10	5	−21.401 (4×10^{-5})	−21.401 (4×10^{-5})	−21.401 (4×10^{-5})
10	10	−21.377 (6×10^{-5})	−21.378 (5×10^{-5})	−21.378 (6×10^{-5})
10	20	−21.308 (7×10^{-5})	−21.309 (8×10^{-5})	−21.309 (6×10^{-5})
10	50	−20.981 (9×10^{-5})	−20.981 (1×10^{-4})	−20.983 (1×10^{-4})
10	100	−20.188 (2×10^{-4})	−20.190 (2×10^{-4})	−20.197 (2×10^{-4})
10	200	−18.076 (3×10^{-4})	−18.075 (4×10^{-4})	−18.100 (4×10^{-4})
10	500	−10.117 (3×10^{-3})	−10.123 (1×10^{-3})	−10.183 (9×10^{-4})

TABLE III. Comparison of the mixing rules MR1 and MR2, used with OFMD, with a direct simulation of the D-Cu mixture for excess pressure and excess internal energy.

	MR1	MR2	Simulation
ρ_D (g cm^{-3})	26.2	20.3	
ρ_{Cu} (g cm^{-3})	67.4	85.8	
P_{ex} (Mbar)	1326.4 (1.0)	1373.1 (1.0)	1340.0 (1.5)
E_{ex} (keV/atom)	−5.1988 (3×10^{-4})	−5.2003 (3×10^{-4})	−5.1962 (3×10^{-4})

steps is necessary because of the different behaviors of deuterium and copper: respectively, kinetic and coupled. We have had to take a smaller time step than the one deduced from Appendix A to reach convergence; apart from the time step, the other numerical parameters are chosen as indicated in Appendix A.

A. Pressure and internal energy

As in Sec. IV, the mixing rules MR1 and MR2, used with OFMD, are applied to the computation of pressure and excess internal energy and compared to direct OFMD simulations. The results are indicated in Table III. The excess pressures given by MR1 and MR2 differ from the excess pressure given by a direct simulation by 1% and 2.5%, respectively; though large in terms of standard deviation, the agreement is good. Excess internal energies agree within a few standard deviations. It can be noted that the same pressures and excess internal energies are obtained (within one standard deviation) with only 45 atoms of deuterium and 5 atoms of copper.

B. Partial ionization and structural properties

OFMD allows one to test prescriptions imposed on the parameters that govern classical models like the one-component plasma (OCP). A comparison of OFMD with the OCP [27] has already been conducted on structural and dynamic properties of iron and gold [8,9]. We carry on with this study by comparing OFMD and the BIM [5] applied to the mixture considered. Like the OCP, the BIM is a parametrized theory that relies on knowledge of effective charges. Usually, the BIM is expressed in terms of effective parameters like the coupling constant. We have chosen to express these effective parameters with the ionizations Z^* provided by the average atom model (and not by OFMD) and the isobaric-isothermal mixing rule [15]; Z^* is defined as the product of the electronic density at the surface of atom j (at T and at the partial density ρ_j) by the volume of atom j. We have found $Z^*=0.89$ for deuterium and $Z^*=11.2$ for copper.

The parameters of the BIM simulation—i.e., number of particles, time step, and number of time steps—are chosen identical to those of OFMD. We perform a simulation of 450 deuterium *ions* and 50 copper *ions* with their respective effective charges, the interaction being in that case purely Coulombic. Ions are propagated during 47 000 time steps in the isokinetic ensemble. The resulting partial pair distribution functions (PDFs) are plotted in Fig. 4. These partial PDFs show the different behaviors of the components, kinetic for deuterium and coupled for copper. The D-D and D-Cu PDFs computed with the BIM are in remarkable agreement with the OFMD simulation. The Cu-Cu PDF obtained with the BIM is slightly more structured than that obtained with OFMD. Yet one must remember that the simulation contains 50 atoms of copper only, which limits the statistical accuracy of our result. Despite this slight difference, our choice of ionizations seems to describe the structural properties correctly.

C. Viscosity

Among transport coefficients used in hydrodynamics, viscosity plays an important role since it governs the development of hydrodynamic instabilities. The viscosity η can be computed from the autocorrelation of the off-diagonal elements of the microscopic stress tensor,

$$\eta = \frac{\beta}{V}\int_0^{+\infty} \eta(t)dt, \tag{11}$$

$$\eta(t) = \frac{1}{3}\sum_{\substack{i,j \\ i>j}} \langle \sigma^{ij}(t)\sigma^{ij}(0)\rangle, \tag{12}$$

where V is the volume, the σ^{ij}'s are the off-diagonal terms of the microscopic stress tensor [28], and $\langle\cdots\rangle$ denotes the av-

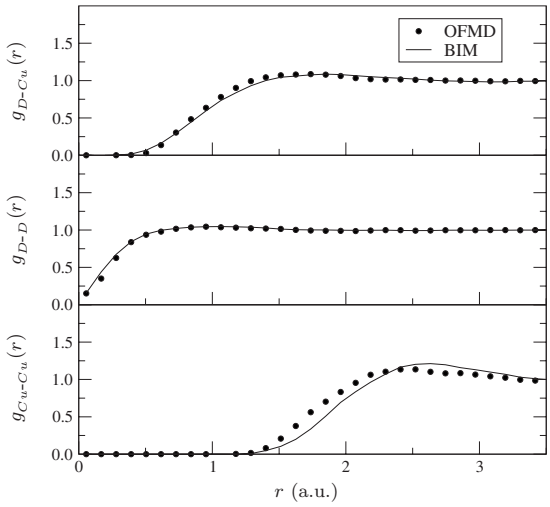

FIG. 4. Partial pair distribution functions of D and Cu in the mixture. Circles represent OFMD results, and lines represent BIM results.

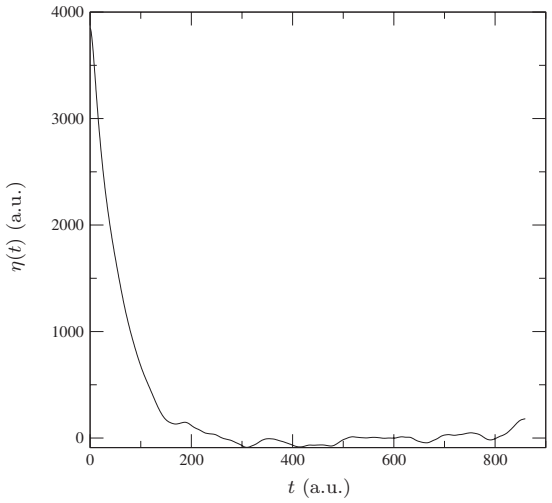

FIG. 5. $\eta(t)$ from the OFMD simulation.

erage in the statistical ensemble considered. The microscopic stress tensor (which has units of energy) is computed for both electronic and nuclear parts [29] with due care to the fact that the kinetic-entropic part of the electronic functional has no contribution to the off-diagonal terms because of the local-density approximation [9].

Since only one value is available at each time step, viscosity is a particularly difficult quantity to compute [5,30] in comparison with diffusion coefficients that are averaged over the particles. This is the reason why we have chosen such a long run for the simulation. The function $\eta(t)$ is plotted in Fig. 5. The time integration in Eq. (11) is carried out on successive 2000-step intervals; the values obtained on each interval are used to calculate the average value and the standard deviation of the viscosity. The statistically noisy part of $\eta(t)$ is replaced by an exponential fit, as already proposed in Ref. [31] for dense matter. We have finally obtained a viscosity $\eta=0.12$ Pa s with a standard deviation of 0.025 Pa s.

1. Mixing rule for viscosity

We have computed with OFMD the viscosity of each pure component at the densities provided by the mixing rules MR1 and MR2 (used with OFMD). Results are summarized in Table IV. The volume fraction of component ℓ is defined, with the notations of Sec. III, by

$$v_\ell = \frac{\rho}{\rho_\ell} \frac{x_\ell A_\ell}{\sum_\ell x_\ell A_\ell}. \tag{13}$$

In the thermodynamic state considered, the viscosity of pure deuterium is driven by kinetic effects whereas the viscosity of copper, because of the coupling, is driven by both potential and kinetic effects; this fact explains the relatively low viscosity of copper. Qualitatively, by comparing the viscosity of the mixture with that of the pure elements, it is obvious that deuterium dominates the behavior of the plasma. Quantitatively, it is interesting to test the validity of a mixing rule for viscosity that is inspired by an effective medium theory and that has already been used in the BIM framework [5].

TABLE IV. Viscosities (η_{MR1} and η_{MR2}) of pure D and pure Cu at $T=100$ eV and at the material densities provided by the mixing rules MR1 and MR2 used with OFMD. Partial densities (ρ_{MR1} and ρ_{MR2}) and volume fractions (v_{MR1} and v_{MR2}) are also indicated.

	D	Cu
ρ_{MR1} (g cm^{-3})	26.2	67.4
ρ_{MR2} (g cm^{-3})	20.3	85.8
v_{MR1}	0.424	0.576
v_{MR2}	0.551	0.449
η_{MR1} (Pa s)	0.30	0.042
η_{MR2} (Pa s)	0.28	0.067

This rule relates the mixture viscosity η_m to the pure-element viscosities η_ℓ and *volume fractions* v_ℓ through

$$\sum_\ell v_\ell \frac{\eta_\ell - \eta_m}{\eta_\ell + \frac{3}{2}\eta_m} = 0. \tag{14}$$

By choosing in Eq. (14) the volume fractions and viscosities at the densities provided by the mixing rules MR1 and MR2 (Table IV), we obtain a mixture viscosity of 0.11 and 0.16 Pa s, respectively, in reasonable agreement with the direct OFMD simulation. It is worth noting that, because of the domination of deuterium, a "simple" mixing rule like serial association $\eta_m = v_D \eta_D + v_{Cu} \eta_{Cu}$ leads to viscosities of, respectively, 0.15 and 0.18 Pa s, which are also fairly close to the OFMD results.

2. What is the information obtained from the direct simulation?

Although statistical uncertainties limit verification of rule (14), it is important to understand that its result relies on knowledge of the volume fractions and pure-element viscosities. Those are obtained through thermodynamic mixing rules so that the adequacy between direct-simulation viscosity and Eq. (14) is largely influenced by the EOS mixing rule. For ideal gases, there exists another EOS mixing rule which is referred to, inappropriately, as the "partial density" mixing rule. Species are assumed not to interact so that $v_\ell = 1$ and

$$\rho_\ell = \rho \frac{x_\ell A_\ell}{\sum_\ell x_\ell A_\ell}. \tag{15}$$

With this mixing rule, partial densities are always less than the total density and entirely independent of temperature. This mixing rule applied to our D-Cu mixture gives partial densities $\rho_D = 11.1$ g cm^{-3} and $\rho_{Cu} = 38.9$ g cm^{-3}. At these partial densities, the viscosities are $\eta_D = 0.24$ Pa s and $\eta_{Cu} = 0.03$ Pa s, and the mixture viscosity obtained with Eq. (14) is 0.09 Pa s; the mixture viscosity obtained with MR1 and Eq. (14)i.e., 0.11 Pa s—is in better agreement with the direct simulation. By providing not only pressure but also volume fractions, the mixing rule MR1 (used with OFMD), along with Eq. (14), gives a reliable result for viscosity in the hot and dense domain.

VI. CONCLUSION

We have applied OFMD to an equimolar mixture of ^{4}He and ^{56}Fe and to an asymmetric mixture of D and ^{63}Cu in the hot and dense regime. We have found that the possibility of computing internal energy with OFMD through Eq. (10), already verified for a pure plasma [10], also holds for mixtures. The isobaric-isothermal mixing rules MR1 and MR2 have turned out to be relevant to calculate pressure and internal energy in the thermodynamic conditions considered; MR1 has also provided parameters allowing the computation of viscosity with Eq. (14). For the computation of pressure and internal energy, the isobaric-isothermal mixing rule dealing with excess pressures (MR1) has given better results than the isobaric-isothermal mixing rule dealing with total pressures (MR2). The two rules yield pressures which become more different as the kinetic pressure due to nuclei becomes a larger part of the total pressure; they yield internal energies which get more different as internal energies depend more on density. Besides, the effective charges given by the isobaric-isothermal mixing rule for the average atom model [15], used in the BIM model, have yielded partial pair distribution functions in good agreement with those given by a direct OFMD simulation. Knowing the effective charges inside the mixture and the validity of the BIM opens new possibilities for the computation of transport coefficients through the fits that exist for the OCP [5,32]. To our knowledge, this work is the first verification of mixing rules in the hot and dense regime in the framework of OFMD as well as the first direct computation of a mixture viscosity without any *ad hoc* prescription like partial ionizations.

ACKNOWLEDGMENTS

We would like to thank Dr. S. Mazevet for fruitful discussions. The present results have been obtained through the use of the electronic structure package ABINIT, a common project of the Université Catholique de Louvain, Corning Inc., and other contributors (URL http://www.abinit.org).

APPENDIX A: COMPUTATIONAL DETAILS

OFMD requires numerical parameters which must be chosen by looking for numerical convergence, within one standard deviation, of the quantity computed. In OFMD, electronic density is expressed as an expansion on a periodic plane-wave basis; the cutoff energy e_{cut} determines the number of plane waves. In order to make this expansion possible, the nucleus-electron interactions are taken as regularized potentials instead of the bare Coulombic potential [8]; these regularized potentials are no longer Coulombic below a given cutoff radius (one for each type of atom). Besides the cutoff energy and the cutoff radii, the main numerical parameters of OFMD are the time step Δt used to displace nuclei, the number N_{time} of time steps, and the number N of atoms in the basic reference cell (infinitely replicated). We choose N_{time} and N by a systematic search for numerical convergence of pressure and internal energy. As in the case of a pure element [10], we have been able to find simple rules allowing a fast determination of the other parameters; these rules are given below.

1. Cutoff radius

It has been shown that, for a plasma with a single type of atom at temperature T and density ρ, a suitable cutoff radius for the computation of pressure and internal energy can be determined from the potential energy of a fcc lattice structure [10]. In the case of a mixture, if $r_{cut,j}$ designates the cutoff radius characterizing the interaction between an electron and a nucleus of type j, we have found that a suitable value of $r_{cut,j}$ is the value of the cutoff radius for a pure plasma with nuclei of type j at temperature T and partial density ρ_j.

2. Cutoff energy

Let $e_{cut,j}$ be defined for each partial density ρ_j and temperature T by the smallest cutoff energy such that

$$\left| \frac{P_{fcc,j}(e_{cut,j}+20)}{P_{fcc,j}(e_{cut,j}+10)} - 1 \right| < 5 \times 10^{-5} \tag{A1}$$

and

$$\left| \frac{P_{fcc,j}(2e_{cut,j}+40)}{P_{fcc,j}(e_{cut,j}+20)} - 1 \right| < 10^{-4}, \tag{A2}$$

where $P_{fcc,j}(e_{cut,j})$ is the pressure calculated with DFT when the nuclei, of type j only, are motionless and located on an fcc lattice structure and when the cutoff energy is $e_{cut,j}$. A suitable value of e_{cut} for the computation of pressure and internal energy of a mixture is the largest of the $e_{cut,j}$'s.

3. Time step

We now turn to the choice of the time step. We define Δt_0 as an adequate time step for the computation of pressure and internal energy obtained, *once and for all*, for an OFMD simulation at ρ_0 and T_0 of a pure element of atomic mass A_0. If A_j is the atomic mass of the element j, the time step Δt_j for a simulation of a pure plasma of j at temperature T and density ρ_j is given by the scaling law

$$\Delta t_j = \left(\frac{T_0}{T}\right)^{1/2} \left(\frac{A_j}{A_0}\right)^{5/6} \left(\frac{\rho_0}{\rho_j}\right)^{1/3} \Delta t_0. \tag{A3}$$

This scaling law is a direct application of a work of Bernu and Vieillefosse on the one-component plasma [33]. It can also be obtained by a rationale similar to that of Ref. [10] dealing with the choice of time step. In the case of a mixture, a suitable value of Δt for the computation of pressure and internal energy is then

$$\Delta t = \sum_j x_j \Delta t_j, \tag{A4}$$

where x_j is the mole fraction of j and Δt_j is calculated with Eq. (A3) and the partial density ρ_j (given by the mixing rule considered).

APPENDIX B: ANOTHER PRESENTATION OF THE MIXING RULES MR1 AND MR2

Let us consider the mixing rule MR2, for instance. It postulates that, once Eqs. (7) and (9) have been solved for the

partial densities ρ_ℓ, the total pressure of the mixture is equal to the common value of Eq. (9) and the excess internal energy per atom is expressed by Eq. (8). In this appendix, we show that we could have obtained the same result by simply postulating, in addition to Eqs. (7) and (9),

$$F(\rho,T,\{x_\ell\}) = \sum_\ell x_\ell F_\ell(\rho_\ell,T), \tag{B1}$$

where, as in the rest of this appendix, the notations of Sec. III are used, and F designates the free energy per atom.

Given the free energy per atom, $F(\rho,T,\{x_\ell\})$, of the mixture, its pressure P is

$$P = \frac{\rho^2}{\sum_\ell x_\ell A_\ell}\left(\frac{\partial F}{\partial \rho}\right)_{T,\{x_\ell\}}. \tag{B2}$$

With Eq. (B1), Eq. (B2) gives

$$P = \frac{\rho^2}{\sum_\ell x_\ell A_\ell}\sum_\ell x_\ell\left(\frac{\partial F_\ell}{\partial \rho_\ell}\right)_T\left(\frac{\partial \rho_\ell}{\partial \rho}\right)_{T,\{x_\ell\}}. \tag{B3}$$

The pressures P_ℓ's can be expressed with the free energy per atom F_ℓ of component ℓ as

$$P_\ell(\rho_\ell,T) = \frac{\rho_\ell^2}{A_\ell}\left(\frac{\partial F_\ell}{\partial \rho_\ell}\right)_T. \tag{B4}$$

Differentiating Eq. (7) with respect to ρ at given T and $\{x_\ell\}$ yields

$$\sum_\ell \frac{x_\ell A_\ell}{\rho^2} = \sum_\ell \frac{x_\ell A_\ell}{\rho_\ell^2}\left(\frac{\partial \rho_\ell}{\partial \rho}\right)_{T,\{x_\ell\}}. \tag{B5}$$

Using Eqs. (9), (B4), and (B5) in Eq. (B3), we obtain

$$P = P_\ell(\rho_\ell,T), \tag{B6}$$

which is the result postulated in the text for the pressure obtained with MR2.

We now consider the internal energy. The entropy per atom of the mixture is

$$S(\rho,T,\{x_\ell\}) = -\left(\frac{\partial F}{\partial T}\right)_{\rho,\{x_\ell\}} \tag{B7}$$

or, with Eq. (B1),

$$S(\rho,T,\{x_\ell\}) = -\sum_\ell x_\ell\left(\frac{\partial F_\ell}{\partial T}\right)_{\rho_\ell} - \sum_\ell x_\ell\left(\frac{\partial F_\ell}{\partial \rho_\ell}\right)_T\left(\frac{\partial \rho_\ell}{\partial T}\right)_{\rho,\{x_\ell\}}. \tag{B8}$$

Differentiating Eq. (7) with respect to T at given ρ and x_ℓ gives

$$\sum_\ell \frac{x_\ell A_\ell}{\rho_\ell^2}\left(\frac{\partial \rho_\ell}{\partial T}\right)_{\rho,\{x_\ell\}} = 0. \tag{B9}$$

Using Eq. (9), (B4), and (B9) in Eq. (B8), we obtain the entropy per atom of the mixture $S(\rho,T,\{x_\ell\})$,

$$S(\rho,T,\{x_\ell\}) = \sum_\ell x_\ell S_\ell(\rho_\ell,T), \tag{B10}$$

$$S_\ell(\rho_\ell,T) = -\left(\frac{\partial F_\ell}{\partial T}\right)_{\rho_\ell}. \tag{B11}$$

With Eqs. (B1) and (B10), the internal energy per atom, $E(\rho,T,\{x_\ell\})$, is equal to

$$E(\rho,T,\{x_\ell\}) = \sum_\ell x_\ell E_\ell(\rho_\ell,T). \tag{B12}$$

Since every nucleus has the same kinetic energy, Eq. (B12) also gives

$$E_{ex}(\rho,T,\{x_\ell\}) = \sum_\ell x_\ell E_{ex,\ell}(\rho_\ell,T), \tag{B13}$$

which is the result postulated in the text for the excess internal energy per atom obtained with MR2.

It can be shown similarly that MR1 can be deduced from Eqs. (6) and (7) and the equality

$$F_{ex}(\rho,T,\{x_\ell\}) = \sum_\ell x_\ell F_{ex,\ell}(\rho_\ell,T), \tag{B14}$$

where F_{ex} designates the so-defined excess free energy—i.e., the free energy minus the free energy of the ideal gas in the conditions considered.

[1] G. Chabrier, D. Saumon, W. B. Hubbard, and J. I. Lunine, Astrophys. J. **391**, 817 (1992).

[2] J. Vorberger, I. Tamblyn, B. Militzer, and S. A. Bonev, Phys. Rev. B **75**, 024206 (2007).

[3] O. Pfaffenzeller, D. Hohl, and P. Ballone, Phys. Rev. Lett. **74**, 2599 (1995).

[4] K. O. Mikaelian, Phys. Rev. E **47**, 375 (1993).

[5] S. Bastea, Phys. Rev. E **71**, 056405 (2005).

[6] J. Clérouin, V. Recoules, S. Mazevet, P. Noiret, and P. Renaudin, Phys. Rev. B **76**, 064204 (2007).

[7] S. Mazevet, F. Lambert, F. Bottin, G. Zérah, and J. Clérouin, Phys. Rev. E **75**, 056404 (2007).

[8] F. Lambert, J. Clérouin, and G. Zérah, Phys. Rev. E **73**, 016403 (2006).

[9] F. Lambert, J. Clérouin, and S. Mazevet, Europhys. Lett. **75**, 681 (2006).

[10] J.-F. Danel, L. Kazandjian, and G. Zérah, Phys. Plasmas **13**, 092701 (2006).

[11] J. P. Hansen, G. M. Torrie, and P. Vieillefosse, Phys. Rev. A **16**, 2153 (1977).

[12] Y. Rosenfeld, Phys. Rev. Lett. **44**, 146 (1980).
[13] G. Chabrier and N. W. Ashcroft, Phys. Rev. A **42**, 2284 (1990).
[14] Y. Rosenfeld, Phys. Rev. E **47**, 2676 (1993).
[15] R. M. More, K. H. Warren, D. A. Young, and G. B. Zimmerman, Phys. Fluids **31**, 3059 (1988).
[16] X. Gonze, G.-M. Rignanese, M. Verstraete, J.-M. Beuken, Y. Pouillon, R. Caracas, F. Jollet, M. Torrent, G. Zérah, M. Mikami *et al.*, Z. Kristallogr. **200**, 558 (2005).
[17] P. Hohenberg and W. Kohn, Phys. Rev. **136**, B864 (1964).
[18] N. D. Mermin, Phys. Rev. **137**, A1441 (1965).
[19] W. Kohn and L. J. Sham, Phys. Rev. **140**, A1133 (1965).
[20] M. Brack and R. K. Bhaduri, *Semiclassical Physics* (Westview Press, Boulder, 2003).
[21] J. P. Perdew and A. Zunger, Phys. Rev. B **23**, 5048 (1981).
[22] F. Zhang, J. Chem. Phys. **106**, 6102 (1997).
[23] P. Minary, G. J. Martyna, and M. E. Tuckerman, J. Chem. Phys. **118**, 2510 (2003).
[24] R. P. Feynman, N. Metropolis, and E. Teller, Phys. Rev. **75**, 1561 (1949).
[25] R. Balian, *From Microphysics to Macrophysics: Methods and Application of Statistical Physics* (Springer-Verlag, Berlin, 2006).
[26] J. L. Milovich, P. Amendt, M. Marinak, and H. Robey, Phys. Plasmas **11**, 1552 (2004).
[27] M. Baus and J.-P. Hansen, Phys. Rep. **59**, 1 (1980).
[28] J.-P. Hansen and I. McDonald, *Theory of Simple Liquids*, 3rd ed. (Academic Press, London, 2006).
[29] O. H. Nielsen and R. M. Martin, Phys. Rev. B **32**, 3780 (1985).
[30] D. Alfe and M. J. Gillan, Phys. Rev. Lett. **81**, 5161 (1998).
[31] F. Ould-Kaddour and D. Levesque, Phys. Rev. E **63**, 011205 (2000).
[32] J. Daligault, Phys. Rev. Lett. **96**, 065003 (2006).
[33] B. Bernu and P. Vieillefosse, Phys. Rev. A **18**, 2345 (1978).